

1
2
3 **The uncertainty of estimating the thickness of soft**
4 **sediments with the HVSR method: A computational point**
5 **of view on weak lateral variations**

6 Article reference: **APPGEO3316**

7 Journal title: **Journal of Applied Geophysics**

8 First/Corresponding author: **Samuel Bignardi Ph.D.**

9 Bibliographic details: **Journal of Applied Geophysics 145C (2017) pp. 28-38**

10 **DOI: [10.1016/j.jappgeo.2017.07.017](https://doi.org/10.1016/j.jappgeo.2017.07.017)**

11
12
13
14
15
16
17 **DISCLOSURE**

18 As defined by the Journal of Applied Geophysics copyright policy, I am allowed
19 to publish my work in its preprint version. The following is the draft/preprint
20 version of the above-mentioned journal article, dated before the first submission
21 for publication. As such, it is slightly different than the final official version.

22 The official version was greatly enhanced in terms of figure legend clarity and
23 overall readability. Further, result presentation was enhanced by summarizing the
24 results in tables (not present here), for a more direct reference. Therefore, the
25 author encourages the interested reader to refer to the official copy, reachable
26 following the link above.

27
28
29
30 **DOI: [10.1016/j.jappgeo.2017.07.017](https://doi.org/10.1016/j.jappgeo.2017.07.017)**

31 **Abstract**

32 The use of the ratio of microtremor spectra, as computed by the Nakamura's technique, was
33 recently proved successful for the evaluating the thickness of sedimentary covers laying over
34 both shallow and deep rocky bedrocks thus enabling bedrock mapping. The experimental
35 success of such application and its experimental uncertainties are today reported in many
36 publications. To map bedrock, two approaches exist. The first is to assume a constant shear
37 wave velocity profile of the sediments. The second, and most preferable, is Ibs-von Seht and
38 Wohlenberg's, based on correlating Nakamura's curves main peak and wells information. In
39 the latter approach, the main sources of uncertainty addressed by authors, despite the lack of
40 formal proof, comprise local deviations of the subsurface from the assumed model. I first
41 discuss the reliability of the simplified constant velocity approach showing its limitations. As
42 a second task, I evaluate the uncertainty of the Ibs-von Seht and Wohlenberg's approach with
43 focus on local subsurface variations. Since experimental basis is well established, I entirely
44 focus my investigation on numerical simulations to evaluate to what extent local subsurface
45 deviations from the assumed model may affect the outcome of a bedrock mapping survey.
46 Further, the present investigation strategy suggests that modeling and inversion, through the
47 investigation of the parameters space around the reference model, may reveal a very convenient
48 tool when lateral variations are suspected to exist or when the number of available wells is not
49 sufficient to obtain an accurate frequency-depth regression.

50

51 **Keywords:** microtremor; HVSr; bedrock mapping; lateral variations; uncertainty

52

53

DOI: [10.1016/j.jappgeo.2017.07.017](https://doi.org/10.1016/j.jappgeo.2017.07.017)

54 **1 Introduction**

55 Since the middle of the last century, the seismic ambient noise has been considered a valuable
56 source of information for the investigation of the shallow subsurface structure. Among other
57 methods, the horizontal to vertical spectral ratio (HVSr or H/V) method (Nakamura, 1989),
58 gained extreme popularity, especially in the last decades in fields such as geology, geotechnics,
59 seismology and recently even in archaeology (Wilken et al, 2015; Abu Zeid et al., 2016, 2017),
60 both because of its simple approach and because it only requires low cost equipment.

61 The HVSr method is based on recording the three components of the seismic noise which are
62 then Fourier transformed and smoothed. The spectral ratio of horizontal to vertical component
63 then, constitutes the so called HVSr (or H/V) curve. The main assumption for the
64 interpretation of such curves is that the subsurface can be well described as a soft sedimentary
65 layer (low shear wave velocity, or V_s) lying over a fast bedrock. In general, both the layer and
66 bedrock are considered homogeneous and viscoelastic, while the seismic noise is assumed to
67 be isotropic. In such a simplified (1-D) model, the correlation between elastic properties,
68 thickness of the sedimentary layer and frequency position of the curve's peaks, has been
69 demonstrated. For example, Lachet and Bard (1994) used a uniform distribution of point-wise
70 sources to numerically simulate the seismic noise in an urban context while Bonnefoy et al.
71 (2006) estimated the effect of different sources on the resulting wavefield. Being an extremely
72 popular topic, the related literature is quite abundant and the interested reader could refer to the
73 study by Bard (1998) who presents an overview of the H/V method, Mucciarelli and Gallipoli
74 (2001), and Deliverables D13.08 (2004), D23.12 (2005) of the European project SESAME.

75 As recalled by Guéguen et al. (2007), the method is used for mainly three different scientific
76 purposes, namely the evaluation of the resonance frequency as correlated to earthquake
77 damage, the investigation of the resonance variation over large areas for microzonation and
DOI: [10.1016/j.jappgeo.2017.07.017](https://doi.org/10.1016/j.jappgeo.2017.07.017)

78 seismic-risk mitigation purposes and finally, for evaluating the thickness of the sedimentary
79 cover or equivalently, the depth of bedrock.

80 Among the three, the evaluation of the sedimentary thickness surely represents the most recent
81 application, so that only a few papers have been published in this area (Ibs-von Seht and
82 Wohlenberg 1999; Delgado et al. 2000; Parolai et al. 2002; Hinzen et al. 2004; Garcia-Jerez et
83 al. 2006; Motamed et al. 2007; D'Amico et al. 2008, Abu Zeid et al. 2014). The bedrock depth
84 (H) could in principle be evaluated using a very simple approach based on the ratio $H = f_0 / \bar{V}_s$
85 between the main resonance frequency f_0 and the average shear wave velocity \bar{V}_s of the
86 sedimentary cover. However, since the problem is posed as an equation with two unknowns,
87 an estimate of the average \bar{V}_s is required. As I will discuss later, this strategy is oversimplified
88 and may lead to severe errors. A preferable approach was described by Ibs-von Seht and
89 Wohlenberg (1999). In their pioneering work, they showed that it is possible to map the
90 thickness of the sedimentary cover by either using an approximate local estimate of the
91 subsurface velocity profile or alternatively, by simply establishing a two-parameters (a, b)
92 regression (sometimes referred to as a calibration function or correlation equation), of the form
93 $H = af_0^b$ which is built using the bedrock depth measured at some existing wells and the
94 resonance frequency f_0 at the well's top, which is obtained by the HVSR method. In their
95 experiment, Ibs-von Seht and Wohlenberg had wells available for roughly 34% of the H/V
96 measurements. Of course, the regression is valid only at the investigated site; but once
97 established it is possible to infer the sediment thickness along the whole survey, provided that
98 the V_s profile presents negligible lateral variation across the surveyed area. It is noteworthy
99 that the calibration function is experimentally determined and does not require an explicit
100 knowledge of the V_s profile. According to experimental evidence, the method proved to be

101 capable of estimating the bedrock depth from shallow targets (less than 50 meters) up to
102 hundreds of meters deep (deep bedrock case).

103 Delgado et al. (2000) examined in depth the theoretical basis of Ibs-von Seht and Wohlenberg's
104 approach in order to better establish the limitations of the method. They concluded that this
105 tool can efficiently be used to retrieve the bedrock depth at locations where this information is
106 missing. Further, as their work was entirely based on field data, they defined the constants of
107 the calibration function for the Bajo Segura Basin (Spain). The bedrock ranged between 15 and
108 60 meters in depth, so their work represents an example of a shallow bedrock situation. Despite
109 the fact that the true sedimentary cover was actually a multi-layered system, which they
110 approximated with just two layers, and despite the topmost sediments were not accounted for,
111 they found that the error in evaluating the bedrock depth was only of on the order of 15% once
112 compared with the available detailed geotechnical information. In this way, they
113 experimentally demonstrated that the general approach is very robust. Further, they discussed
114 different sources of uncertainty that may affect the depth estimates and addressed local lateral
115 subsurface deviations from the assumed velocity profile as the main source of error.

116 Using Ibs-von Seht and Wohlenberg's regression, Parolai et al. (2002), found a systematic
117 underestimation (up to 30%) in the thickness estimates performed in the Cologne area
118 (Germany), with the largest error corresponding to those areas of deepest bedrock. They
119 concluded that the Ibs-von Seht calibration curve was not suitable for the area at hand and
120 derived a new set of parameters capable of reducing such error.

121 Gosar and Lenart (2010) gave a comprehensive overview of the regression parameters values
122 encountered in literature. Further, they applied the method for the Ljubljana Moor Basin
123 (Slovenia). They had a good availability of wells and their f_0 -H regression was based on 53
124 unevenly distributed wells. Such regression was then used to retrieve the bedrock depth along

DOI: [10.1016/j.jappgeo.2017.07.017](https://doi.org/10.1016/j.jappgeo.2017.07.017)

125 an independent profile. They gave a detailed discussion about experimental uncertainties
126 mainly addressing 2D and 3D effects due to the basin geometry and local lateral variations.
127 Further they pointed out the presence of side peaks as an indication of the presence of a
128 complex subsurface structure.

129 Finally, Johnson and Lane (2016) compared different methods of evaluating the thickness of
130 sediments using field data and a statistical approach. They investigated a shallow bedrock case
131 (depth ranged between 1 and 60 meters), and in that context, they compared the bedrock depth
132 obtained by a purposely derived calibration function, two third-party calibration functions and
133 the one obtained using the simplified constant V_s approach (equation 2). Noteworthy, from
134 their work it can be observed that the bedrock depth obtained using the constant average V_s
135 approach, when compared to that obtained by the ad-hoc produced calibration function, is
136 systematically underestimated. The underestimation increased with depth reaching roughly
137 15% in the worst case scenario.

138 Judging from published experimental evidence, therefore, it is quite established that this
139 application of HVSR is very robust, provided that a purposely built calibration function is
140 available for the site at hand. Evaluation of experimental uncertainties shows that in general,
141 when compared with wells data, the error in bedrock depth estimates is lower than or at least
142 comparable to 15 percent. Authors have justified this discrepancy invoking different sources
143 of uncertainty with local lateral variation of elastic properties as the most popular one, despite
144 the lack of formal proof. Since experimental evidence about the success of the method and its
145 degree of uncertainty are already very convincing, the purpose of this paper is not the
146 evaluation of uncertainties through the study of further experimental datasets. I will rather
147 investigate the lateral variation exclusively from a modeling point of view.

DOI: [10.1016/j.jappgeo.2017.07.017](https://doi.org/10.1016/j.jappgeo.2017.07.017)

148 The way a lateral variation changes the outcome of the bedrock depth estimation is that a slight
149 local change in subsurface elastic properties results in a small shift of the resonance frequency.
150 We can then imagine the lateral variation as a small perturbation of our reference model,
151 compute the resonance frequency of the perturbed model and evaluate how the frequency shift
152 affects the estimated depth. Since with a given a reference model there are an infinite number
153 of possible perturbations, a statistical approach must be used.

154 To accomplish this I used a modified version of the code OpenHVSr v2.0 (Bignardi et al.
155 2016, Herak, 2008), which allows the simulation of HVSr curves either considering the
156 contribution of body waves, implemented using Tsai and Housner's approach (Tsai, 1970; Tsai
157 and Housner, 1970) and surface waves, through the approach implemented by Lunedei and
158 Albarello (2010) as the formation mechanism. Indeed, it was demonstrated (Nakamura, 2000;
159 Bonnefoy et al. 2006) that the seismic noise may contain contributions from both multiple
160 refracted body waves and surface waves; so that, for consistency, both formation mechanisms
161 must be investigated. Two different multi-layered subsurface scenarios are used as reference.
162 The first is a multi-layered system with a constant V_s profile, while the second implements the
163 same velocity-depth distribution discussed in the paper by Ibs-von Seht and Wohlenberg
164 (1999), which is a normally dispersive model accounting for the confinement pressure
165 increasing with depth. The investigation is performed by using the Montecarlo method (MC)
166 to produce a statistically meaningful number of perturbations of the reference models. I
167 randomly perturbed both the V_s and V_p profiles evaluating the impact of the introduced
168 perturbation on the resonance frequency and the consequent impact on the estimated thickness
169 of sediments.

170

171

DOI: [10.1016/j.jappgeo.2017.07.017](https://doi.org/10.1016/j.jappgeo.2017.07.017)

172 2 Material and methods

173 All tests performed here were realized using an ad-hoc modified version of the program
174 OpenHVSR (Bignardi et al., 2016) specifically designed for bedrock depth evaluation
175 purposes. Each test investigated a different reference subsurface configuration. The first one
176 (Table A.1) built using a constant V_s profile subdivided in 5 layers, each one 8 m thick,
177 simulates a soft sedimentary cover lying over a hard half space. Two different sets of models
178 were produced by perturbing this reference subsurface in order to obtain a set of normally
179 dispersive and a set of inversely dispersive models, all produced by keeping the thickness of
180 layers constant. Consequently, the depth of bedrock was fixed at 40 meters depth. As such, this
181 represents a shallow bedrock scenario. Perturbations consisted of changing the V_s velocity of
182 each layer by a random amount, up to 50% variation with respect to the original value under
183 the requirement that the whole perturbed profile must present the same average V_s as the
184 reference model, when calculated according to

$$185 \quad V_{ave} = \frac{\sum_i H_i}{\sum_i \frac{H_i}{V_i}}, \quad (1)$$

186 where H_i and V_i are the thickness and velocity of the i^{th} layer respectively. Prior to being
187 applied, perturbations were ordered in ascending or descending order to generate the normally
188 or inversely dispersive behavior.

189 When the subsurface can be described with one whole slow layer over a fast half space, the
190 elastic wave equation can be analytically solved in term of resonance frequencies. The quite
191 popular solution states that the H/V curve shows many peaks occurring at the resonance
192 frequencies of the system (Lanzo, 1999). Further, these frequencies only depend on the shear
193 velocity V_s and thickness H of this single layer (equation 2)

194 $f_{(n)} = \frac{V_s}{4H} (2n - 1) ,$ (2)

195 where n indicates a specific peak of the H/V curve. If the half space is partially adsorbing, the
196 amplitude of the peaks is decreasing when n increases, so that usually, only the main peak ($n =$
197 1) is considered. This disarmingly simple result is easily proven by assuming the multiple
198 reflection and refraction of shear waves (Lanzo, 1999). Of course, if the V_s profile can be
199 determined, equation 2 could, in principle, be used to infer the depth of bedrock, and if multiple
200 measurements are available over the same area, the bedrock may even be mapped.

201 However, from a modeling point of view, the subsurface is better described as a stack of layers
202 with properties changing with depth which in turn requires enforcing stress and displacement
203 continuity conditions at the interfaces between layers. For this reason, the solution of a
204 multilayered system is inherently different when compared to the solution of the unique-layer
205 over half space model and H/V curves must be computed numerically. It could be argued that
206 the effect of such interface conditions is negligible when the change in elastic properties is
207 small, and especially, when such changes are small compared with the abrupt elastic impedance
208 contrast at the sediments-bedrock interface. This is a reasonable observation, and as a matter
209 of fact, many authors still use equation (2) to obtain a rough evaluation of the bedrock depth.
210 Yet, to my knowledge, no theoretical investigation has been carried out in this direction.
211 Therefore, the purpose of my first test is to numerically quantify the expected deviations which
212 may affect the bedrock depth estimate when the latter are performed by the simple but arguable
213 application of equation 2.

214 My second test concerns the evaluation of the impact of subsurface deviations from a defined
215 reference model, which is represented by a more sophisticated subsurface built using a V_s
216 profile defined through equation 3

$$H = \left[\frac{V_0(1-x)}{4f_r} + 1 \right]^{1/(1-x)} - 1, \quad (3)$$

which relates the thickness of sediments H to the resonance frequency f_r and accounts for the increase of V_s with depth due to the increasing confining pressure. I set $V_0 = 162$ m/s as the shear wave velocity at the surface and $x = 0.278$ as depth-weighting constant so obtaining the same model investigated by Ibs-von Seht and Wohlenberg (1999). Further, the V_p profile is built to account for both the augmented velocity with depth and to accommodate the water table (WT). See tables A.2 and A.3 for details.

Ibs-von Seht and Wohlenberg demonstrated that by knowing the bedrock depth at a sufficient number of locations (through wells or other geophysical methods) and computing the main resonance frequency by the HVSR method at the same locations, a regression of the form $H = af^b$ can be built. Such regression can then be used to map the sediment thickness over the entire areas under investigation, without the need of determine the V_s profile, provided that the shear velocity profile obeys a relation similar to equation 3 and without lateral variations.

Therefore, as a first step, I evaluated the parameters a and b for the reference model described by equation 3 simulating the H/V curves for different bedrock depths, under both the assumption of the body and surface waves formation mechanism. The result is compared with Ibs-von Seht and Wohlenberg's original work and other published analogous work in table 1.

Site	Regression	a	b
Cologne (Germany)	Parolai et al. (2002)	108.0	-1.551
Lower Rhine-east (Germany)	Hinzen et al. (2004)	137.0	-1.190
Lower Rhine-west (Germany)	Ibs-von Seht and Wohlenberg (1999) field data	96.0	-1.388
	Ibs-von Seht (1999) Theoretical	111.52	-1.3677
This Study	Body Waves (Tsai...)	133.41	-1.2615
	Surface Waves (Picozzi...)	140.40	-1.4077

234 **Table 1:** Regression parameters a and b published in different case studies as compared with
235 those numerically computed in this investigation

236 I recall that the purpose of this second investigation was to evaluate the amount of uncertainty,
237 due to a lateral variation, which could affect the sediments thickness evaluation. According to
238 published work, such uncertainty depends both on the depth at which the real subsurface
239 deviates from the assumed model and on the depth of bedrock. Since in the majority of
240 publications regarding this topic the assumption of no lateral variation is a good approximation
241 for the most part of the measurement locations, it seems reasonable that such variations take
242 the form of a local lens having changed elastic properties. Following these considerations I
243 investigated two cases in which the bedrock lies 750 and 50 meters deep, which represent deep
244 and shallow bedrock scenarios respectively. The subsurface for the two scenarios was
245 subdivided respectively into 32 and 18 layers and successively used to generate six different
246 sets of perturbed models each. The effect of shallow, middle-depth and deep perturbations was
247 investigated by changing the velocity values in the topmost, central and deep portion of layers
248 respectively.

249 Further, to simulate the effect of a lenticular body crossing the model under the measurement
250 point, each velocity perturbation was built by generating random values with normal
251 distribution and ordered so as to obtain a vector of values with the maximum in the middle
252 position and symmetrically fading. Such perturbation was then added to or subtracted from the
253 velocity values of the portion of layers at hand to investigate both the velocity underestimation
254 and overestimation. For clarity sake, a few selected perturbed models are shown later in figure
255 4. The same strategy was used both to modify V_s and V_p .

256 However, two independent perturbation vectors were generated each time as I wanted to keep
257 V_p and V_s uncoupled. Indeed, despite the fact that the V_p parameter has a weak effect on the
DOI: [10.1016/j.jappgeo.2017.07.017](https://doi.org/10.1016/j.jappgeo.2017.07.017)

258 H/V curve when compared to V_s (Bignardi et al., 2016), its importance should not be
259 overlooked. In particular, I introduced the water table effect as a constant $V_p=1500$ m/s
260 extending from the shallow layers to a depth where this value was reasonably exceeded.

261 Finally I allowed a maximum layer-wise variation of 50% for velocities, while density and
262 quality factors were kept constant. All parameters of the bedrock were kept fixed as well.

263 Of course, every perturbed subsurface presented slightly changed average values of both V_s
264 and V_p with respect to the reference model, and consequently, slightly different resonance
265 frequency. Therefore, the percent change in average V_s was correlated to the percent change in
266 the resonance frequency. Further, the error in evaluating the bedrock depth was estimated and
267 correlated to the average V_s as well.

268 The chosen amount of perturbations could not entirely change the nature of the model defined
269 by equation 3, so that the perturbed models retained an almost normally dispersive trend in
270 nature. Consequently, I classified different sets of simulations based on the characteristics of
271 the perturbation used: “shallow”, “middle-depth” and “deep”, depending on the position of the
272 affected layers, and “+”, or “-” when velocities were increased or decreased.

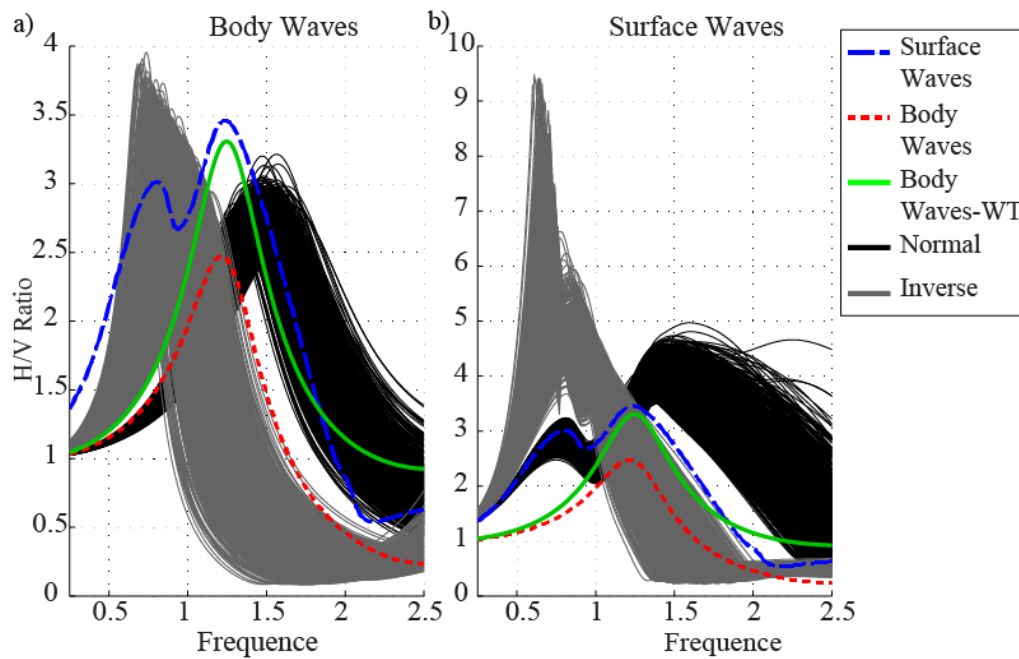
273 Concerning the modeling routines I used, since the computational time required to run the
274 surface waves-based one is consistently slower than the body waves-based one, the number of
275 perturbed models I produced using the first is smaller with respect those produced using the
276 second one. Therefore, in both the first and second test, the datasets related to body waves
277 comprised 50,000 subsurface perturbations while the simulation of surface waves comprised
278 5,000. As a final consideration regarding test 2; it could be argued that, the use of modeling
279 routines based on a subsurface described by a stack of flat layers to investigate lateral variations
280 seems like a contradiction. Indeed, such approach is only valid under the assumption that the

281 local lateral variation is small compared to the wavelength associated to the main peak, which
282 is indeed the case of the present simulation, as the perturbed portion of the subsurface spanned
283 over few layers.

284 **3 Results**

285 **3.1 Test one:**

286 In my first test, the subsurface model of table A.1 was perturbed using the MC approach in
287 order to produce two different sets of models. I investigated a set of perturbations where the
288 resulting subsurface is strictly normally dispersive and a second set which is strictly inversely
289 dispersive. Since the V_p profile has a weak, but not negligible impact on the main peak
290 position, each time a V_s subsurface is created, a corresponding V_p profile is created using an
291 extra MC run. This allowed an investigation of the perturbed models with variable V_p/V_s ratios
292 so that the final result of the investigation is free from effects that may be addressed to a
293 systematic use of a linear dependence between the two elastic parameters. As a perturbed
294 subsurface generates an H/V curve with a main peak slightly changed in position, only a
295 limited range of frequencies need to be investigated. Figure 1a and 1b show the H/V curve
296 obtained considering body and surface waves respectively. The response of the reference model
297 for body waves with or without the presence of the water table is represented by the thick solid
298 and the narrowly dashed lines respectively, while the loosely dashed line corresponds to the
299 response of surface waves.



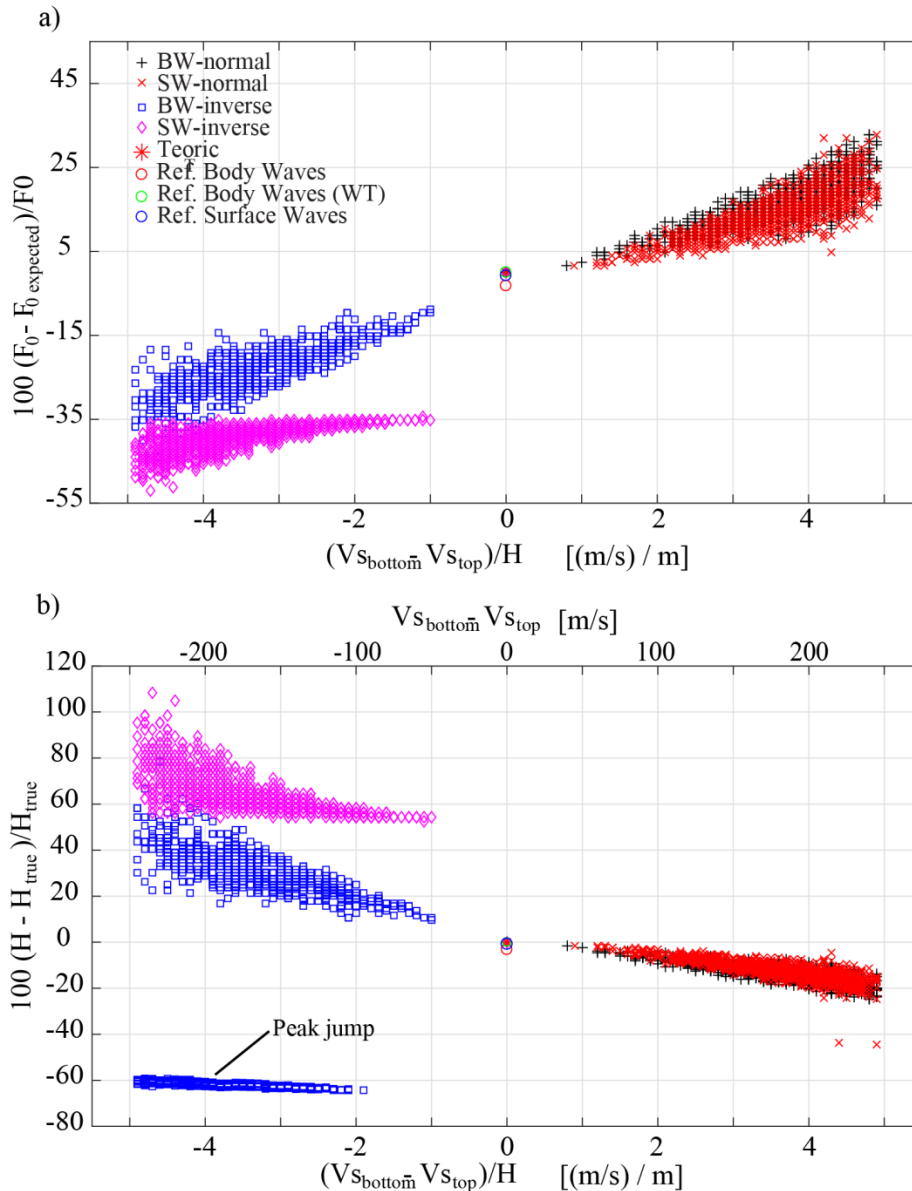
300

301 **Figure 1:** H/V curves simulated using the propagation of body and surface waves are shown
 302 in figures a) and b) respectively. The reference model response when the body-waves formation
 303 mechanism is considered is shown with a solid and a narrowly dashed line, depending if the
 304 water table effect is included or not, while the response of surface waves (water table included)
 305 is shown with the loosely dashed line. The sets of black and gray lines represent the responses
 306 of normally and inversely dispersive models respectively. All the investigated models share the
 307 same depth to bedrock and the same average V_s .

308 The curves obtained for the normally and inversely dispersive perturbed models are shown in
 309 black and gray respectively. The figure shows that despite that the average V_s is the same for
 310 all the models, the frequency of the main peak is systematically overestimated (underestimated)
 311 when the subsurface becomes a multilayered normally (inversely) dispersive system. The
 312 behavior seems to be accentuated for the surface waves which in this particular subsurface
 313 configuration may undergo a jump of peak, i.e. a peak that is secondary for the reference model
 314 becomes dominant for the perturbed subsurface. Figure 2a shows the percent difference

DOI: [10.1016/j.jappgeo.2017.07.017](https://doi.org/10.1016/j.jappgeo.2017.07.017)

315 between the frequency peak positions of the perturbed models with respect to the expected
 316 value, as a function of the average velocity gradient of the corresponding subsurface.



317

318 **Figure 2:** a) The percent difference between the frequency position of the main peak of the
 319 H/V computed for the reference model and the corresponding position of peaks obtained for
 320 the perturbed models is shown as a function of the average velocity gradient of the
 321 corresponding subsurface. In the legend, abbreviations “BW”, “SW”, “Ref” and “WT” stand

DOI: [10.1016/j.jappgeo.2017.07.017](https://doi.org/10.1016/j.jappgeo.2017.07.017)

322 for “Body waves”, “Surface Waves”, “Reference model response” and “accounting Water
323 Table” respectively. b) Percent difference in estimated sediment thickness with respect to the
324 known value is shown as a function of the average V_s gradient (scale at bottom) and as a
325 function of the V_s difference between the bottom and the top sediments (scale on top).

326 When the subsurface is normally dispersive, the deviation is almost always bounded under
327 30%. For the inversely dispersive case, body waves mostly lead to a deviation under 35%, but
328 in some cases it is possible for the main peak position to change abruptly. The latter gives rise
329 to a cloud of points which, for clarity sake, I decided not to show in figure 2a. However its
330 effect on thickness error is shown in figure 2b. Surface waves, as it can be noted, are greatly
331 affected by the inversely dispersive subsurface.

332 Figure 2b shows the percent difference in estimated sediment thickness (using equation 2) with
333 respect to the known value as a function of both the average V_s gradient (scale at bottom) and
334 as a function of the velocity difference between the bottom and the top of sediments (scale on
335 top).

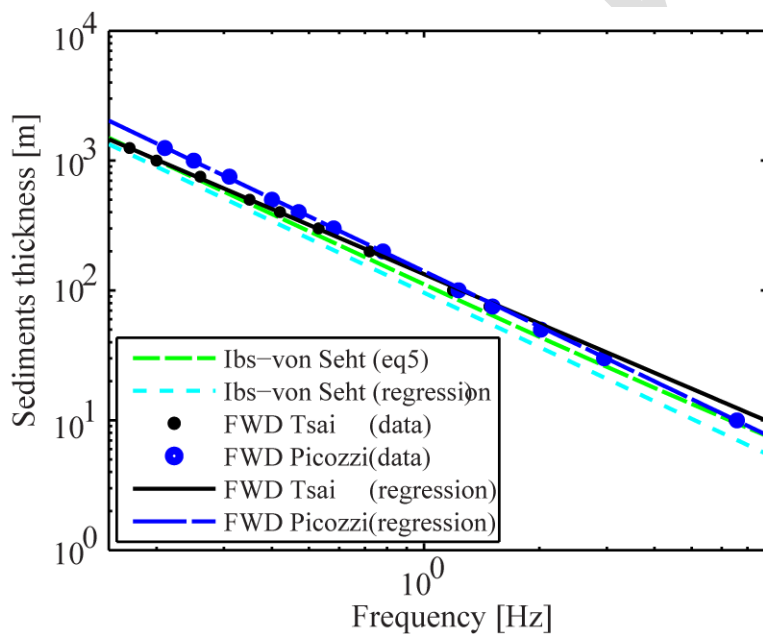
336 For the normally dispersive subsurface case, the error in subsurface sediments thickness
337 evaluation is mostly under 30 percent, even in the most extreme case.

338 For inversely dispersive models, body waves lead to an error under 20% only when the
339 inversion is weak while in cases of strong inversion may lead to an error up to 40-60% or to
340 abrupt changes of main peak position and consequently the sediment thickness may be severely
341 mistaken. It is worth mentioning that the latter conclusion only apply when the whole profile
342 is inversely dispersive which seldom happens in real soils, while the case of inversion limited
343 to few layers, as it will be show in the following, behaves much more regularly. It is worth
344 noting that when the constant V_s subsurface is used as reference and we change toward a

345 normally dispersive one, the consequence is depth underestimation. Conversely, if the normally
346 dispersive subsurface is taken as the true model, switching towards a constant V_s one results in
347 depth overestimation. This is exactly what experimentally was obtained by Johnson and Lane
348 (2016) who found that the constant V_s approach lead to a shallower bedrock depth when
349 compared to that obtained by the Ibs-von Seht and Wohlenberg – like regression.

350 3.2 Test two

351 As first part of my second test, the V_s profile of equation 3 was used to computationally obtain
352 the parameters a and b of the Ibs-von Seht and Wohlenberg fashioned regressions shown in
353 figure 3.



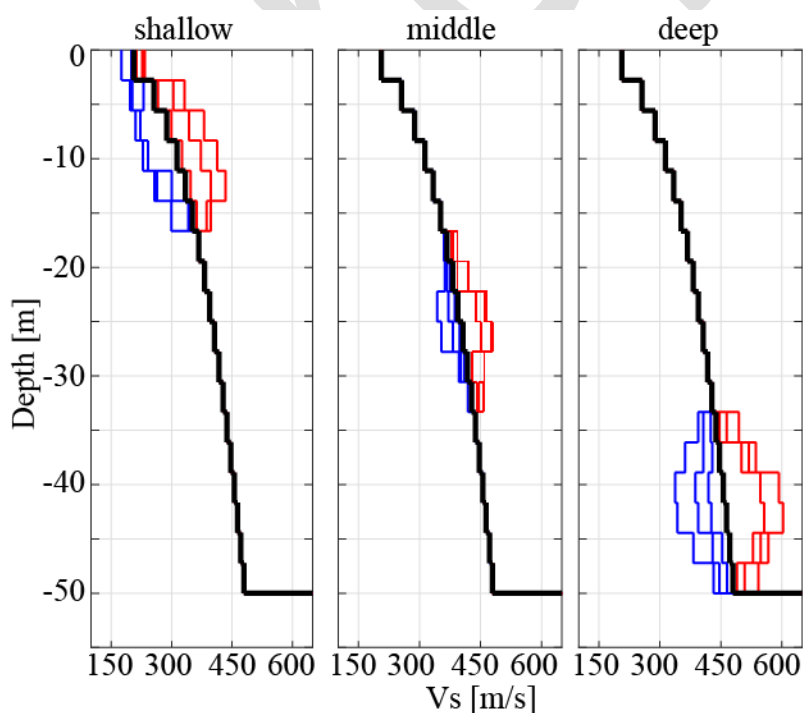
354

355 **Figure 3:** Comparison between regressions. Ibs-von Seht and Wohlenberg’s analytical
356 calibration curve (Ibs-von Seht and Wohlenberg 1999, equation 5) and empirical regression are
357 compared with the regressions obtained in this study and simulated (f_r, H) points, as obtained
358 for Ibs-von Seht and Wohlenberg’s (1999) subsurface model (equation 3) and computed
359 assuming both the body and surface waves propagations as formation mechanisms.

DOI: [10.1016/j.jappgeo.2017.07.017](https://doi.org/10.1016/j.jappgeo.2017.07.017)

360 The regressions based on body and surface waves propagation are drawn in solid black and
361 loosely dashed blue respectively. Such regression lines are based on specific simulations
362 highlighted with circles in the figure and performed using Tsai and Housner's approach (for
363 body waves) and Picozzi and Alarello's approach (for surface waves). Ibs-von Seht and
364 Wohlenberg's regressions are shown alongside for comparison. Finally, values for a and b
365 constants for different regressions commonly encountered in literature are listed in table 1.

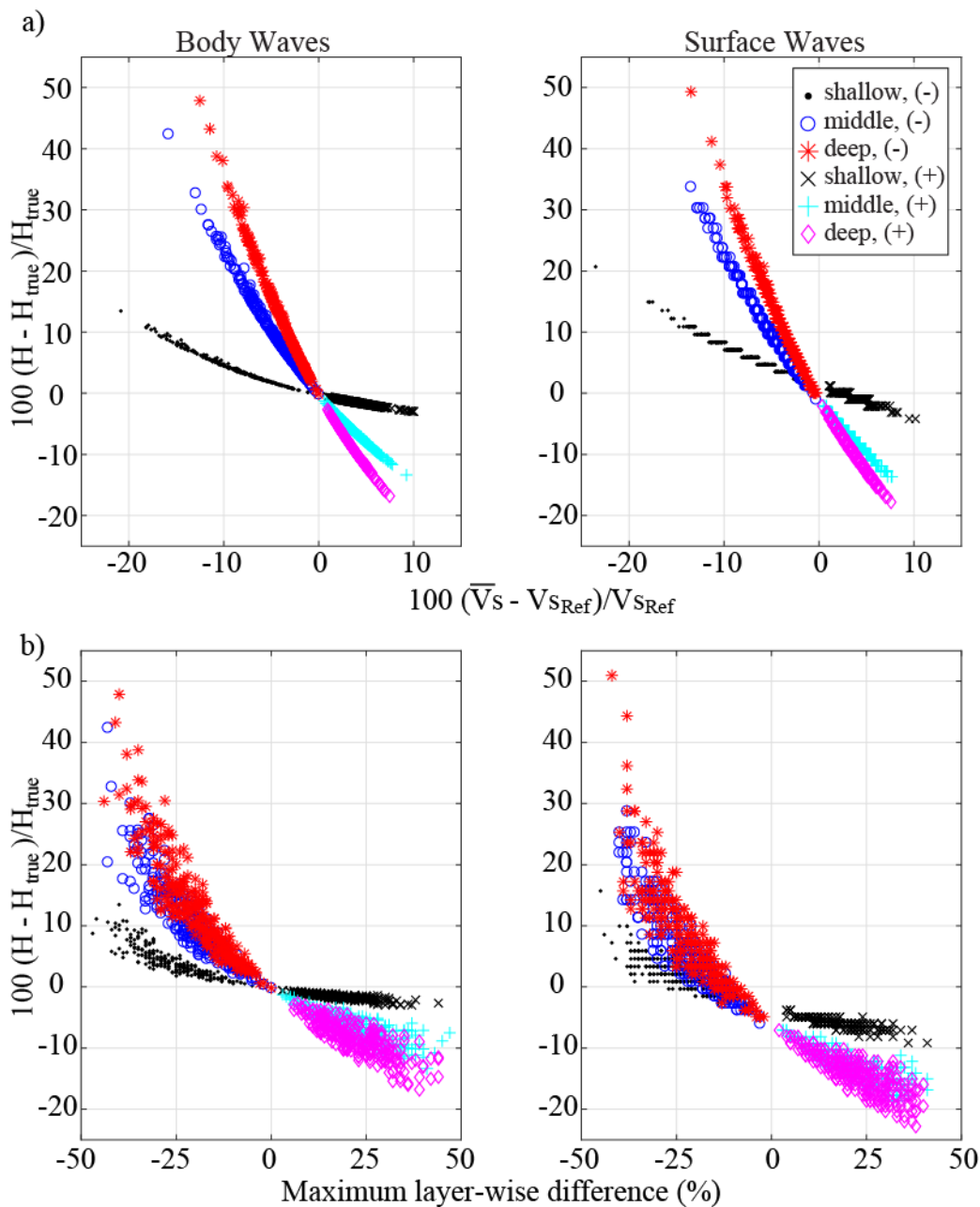
366 In the second part of the present investigation, a Monte Carlo algorithm was used to obtain,
367 from the two models of tables A.2 and A.3, three different sets of perturbed models by
368 perturbing a portion (one third) of the layers at time. The first, second and third set were
369 obtained by perturbing the shallow, middle and deep portion respectively. The perturbation
370 strategy consisted in slightly changing both V_s and V_p to obtain a perturbation symmetric with
371 respect to the perturbed section with its maximum change in the middle and fading toward the
372 edges (few selected examples are shown later on, in figure 4. Such perturbations were either
373 added or subtracted in order to investigate both the cases of velocity



374

DOI: [10.1016/j.jappgeo.2017.07.017](https://doi.org/10.1016/j.jappgeo.2017.07.017)

375 **Figure 4:** Few selected examples of subsurface perturbation, (shallow bedrock), designed to
 376 study the dependence of the error in bedrock depth evaluation resulting by a shallow, middle-
 377 depth or deep change in velocity.
 378 overestimation and underestimation. Figures 5a and 5b, related to the case of shallow bedrock
 379 (50 m deep), show the percent error in evaluating the sediment thickness as compared to the
 380 average V_s velocity of the entire stack of layers and to the maximum layer-wise variation.



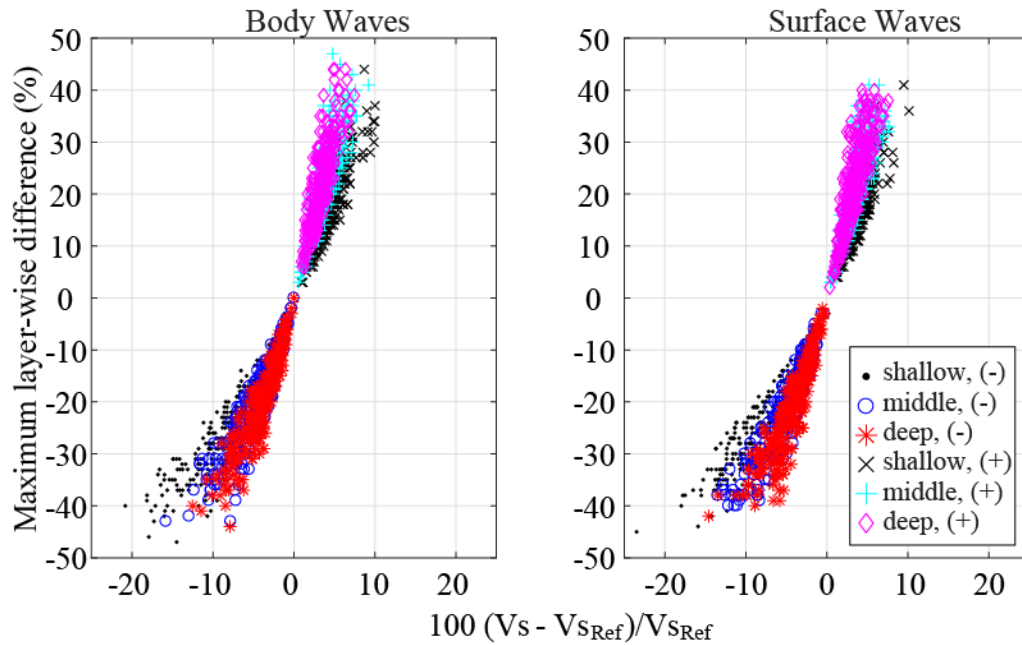
381

382 **Figure 5:** The percent difference between the bedrock depth evaluated using the H/V main
383 peak and the computed regressions (figure 3), and the true value (50 m), is shown as a function
384 of the average V_s of the subsurface (a) and as a function of the maximum layer-wise V_s
385 perturbation (b). Effects of both body and surface waves formation mechanisms were
386 investigated.

387 Note that, in this example the sediment thickness was evaluated, congruently with Ibs-von Seth
388 and Wohlenberg's approach using the regression previously obtained (figure 3).

389 The result for all of the three subsurface sections and for both the velocity underestimation and
390 overestimation scenarios is plotted. It can be noted that, in general, the average V_s variation is
391 limited under 20% and in this range when the average velocity is increased, the percent error
392 is under 15%. On the other hand, in case of velocity underestimation, the error is still limited
393 but can be higher. The cases of shallow, middle-depth and deep perturbation show a similar
394 behavior, except that the effect is stronger when the varied layers are deeper. This is because
395 even if a generic change of V_s affects the whole profile, when such change is deeper it has a
396 greater effect on low frequencies where the resonant peak usually lies. Shallow perturbations,
397 on the other hand, affect mostly (but not only) the high frequency part of the curve. Surface
398 waves and body waves formation mechanisms behave coherently. Figure 5b shows the
399 estimated percent error in sediment thickness as a function of the maximum percent layer-wise
400 change. It seems that to obtain an error of about 15%, a subsurface V_s variation higher than
401 25% is required. Bearing in mind how the lens was simulated in this study, such variation can
402 be considered rather strong, and this explains why the errors addressed to lateral changes in the
403 literature are usually of the order of 15% or less.

404 Finally, for sake of completeness, figure 6 relates the percent change in average V_s velocity
405 with the percent maximum layer-wise variation. It can be noted that the impact on the average
406 V_s of changing the V_s of few layers is modest even when such change is consistent.

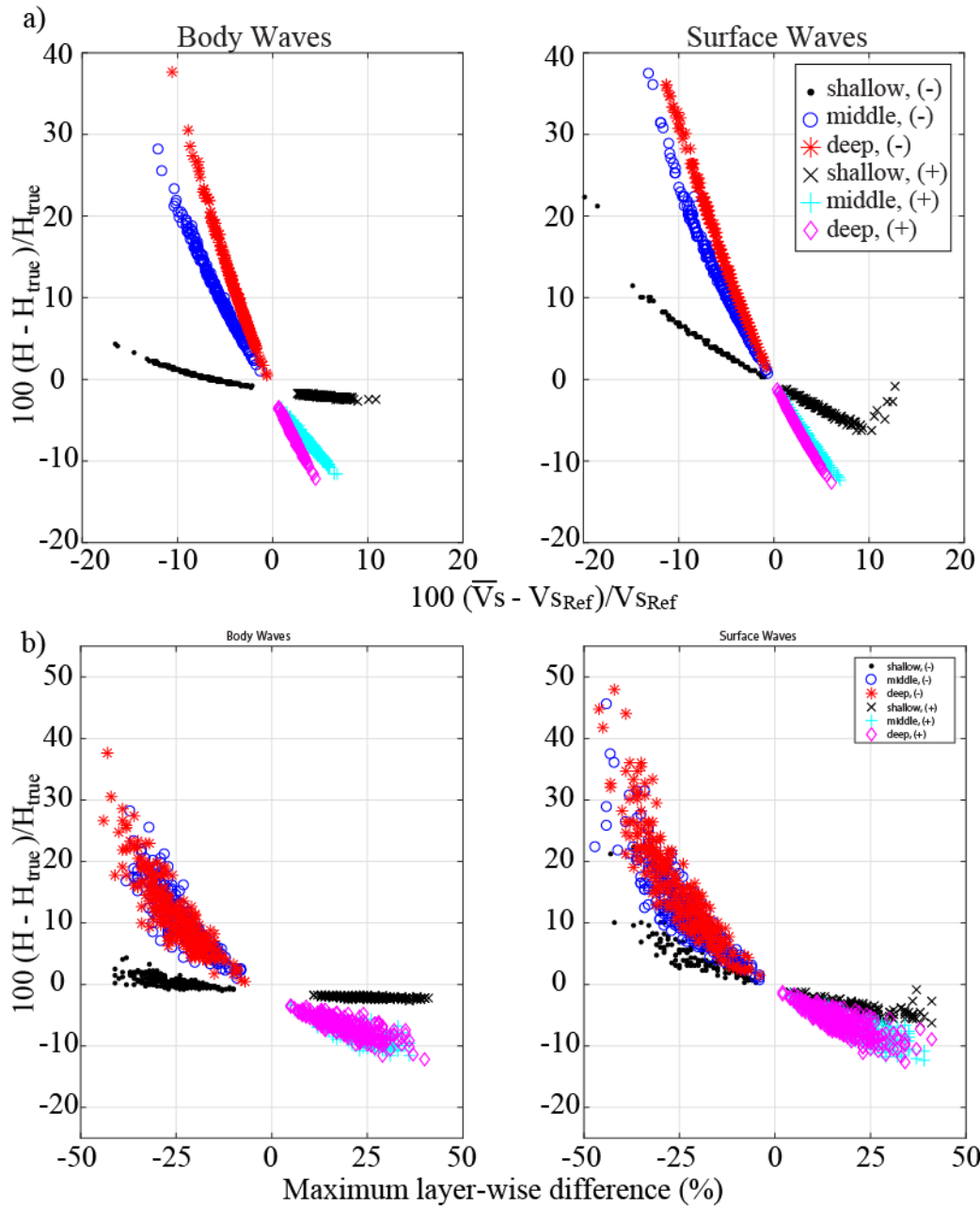


407

408 **Figure 6:** Average V_s of the subsurface as a function of the maximum layer-wise V_s
409 perturbation for a bedrock 50 m deep.

410 As a result Ibs-von Seht and Wohlenberg's approach results particularly stable against local
411 lateral variations.

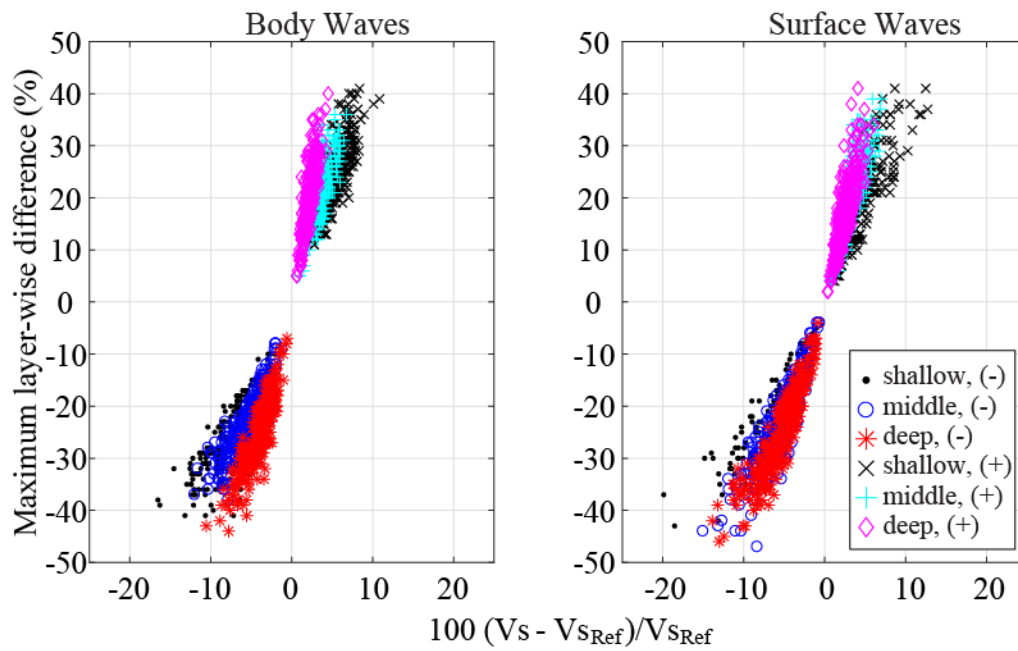
412 Figures 7 and 8 show the analogs of figures 5 and 6 in the case of deep bedrock (750 m).



413

414 **Figure 7:** The percent difference between the bedrock depth evaluated using the H/V main
 415 peak and the computed regressions (figure 3), and the true value (750 m), is shown as a function
 416 of the average Vs of the subsurface (a) and as a function of the maximum layer-wise Vs
 417 perturbation (b). Effects of both body and surface waves formation mechanisms were
 418 investigated.

DOI: [10.1016/j.jappgeo.2017.07.017](https://doi.org/10.1016/j.jappgeo.2017.07.017)



419

420 **Figure 8:** Average V_s of the subsurface as a function of the maximum layer-wise V_s
 421 perturbation for a bedrock 750 m deep.

422 The same considerations made for the shallow bedrock case hold except the effect of perturbing
 423 the shallow portion of the velocity profile is rather limited, as could be expected. Such low
 424 impact of the shallow part of the velocity profile explains why Delgado et al. (2000) were able
 425 to overlook the topmost soil without affecting their final result.

426 For the deep bedrock case, the error related to surface waves seems to be slightly higher than
 427 the one obtained for body waves. However, such a difference could be simply due to the
 428 different computational approach implemented in the forward modeling routines and it seemed
 429 not sufficiently pronounced to suggest any special physical interpretation. As was pointed out
 430 in test 1, the use of the simplified approach of equation 2 for the determination of H , even
 431 calculating the average V_s from the true profile (equation 1), always led to underestimation.
 432 The error, both considering body or surface waves, was about 9% for the shallow bedrock case,
 433 while was of 3% (body waves) and 22% (surface waves) for the deep bedrock scenario.

DOI: [10.1016/j.jappgeo.2017.07.017](https://doi.org/10.1016/j.jappgeo.2017.07.017)

434 **4 Conclusion**

435 It is known from experimental evidence that the HVSR method has proved to be successful for
436 mapping the thickness of sedimentary covers laying over rocky bedrock.

437 The simplest approach based on constant V_s (equation 2) reveals to be an oversimplified
438 strategy which on the most common realistic case, i.e. a normally dispersive subsurface with
439 V_s increasing with depth, may lead to systematic underestimation of the bedrock depth on the
440 order of 15-25%. This conclusion was shown by experimental evidence in the work by Johnson
441 and Lane (2016). Conversely, when the subsurface is entirely inversely dispersive, the error
442 may easily exceed 20%. Further error may arise when a secondary peak exists because such a
443 peak may become dominant as a result of the lateral variation. Despite the fact that only a
444 “shallow bedrock” scenario was investigated, my results point out that the use of the simplified
445 approach of equation 2 should be used with care and only to gain a rough understanding of the
446 subsurface.

447 A far more elegant and reliable approach was described by Ibs-von Seht and Wohlenberg
448 (1999), in which a site dependent calibration function is built and used for the bedrock depth
449 estimation. I numerically computed the theoretical calibration functions for both the cases in
450 which the H/V curve is to be considered as the outcome of multiple reflected and refracted
451 body waves or as the result of surface waves propagation. Despite the fact that two independent
452 modeling routines and two independent formation mechanisms were considered, the result,
453 computed for the same subsurface model revealed to be very similar to that proposed by Ibs-
454 von Seht and Wohlenberg. Since in this contest, among the various sources of uncertainty that
455 can affect the sedimentary thickness estimation, the local deviations from the assumed model
456 have been suggested by many authors as the most contributing factor, I numerically
457 investigated this aspect for the Ibs-von Seht and Wohlenberg’s subsurface model taking into
DOI: [10.1016/j.jappgeo.2017.07.017](https://doi.org/10.1016/j.jappgeo.2017.07.017)

458 account shallow (50 m) and deep (750 m) bedrock scenarios. In both cases the introduction of
459 localized perturbations in soil velocities produced results in line with the experimental
460 observations. In particular, the deeper the perturbation, the stronger was the resulting error on
461 thickness. Further, an increase (decrease) of V_s systematically led to depth underestimation
462 (overestimation).

463 I verified that, in both cases, subsurface variations capable of changing the average V_s up to
464 10% may at most introduce errors of 20% or less in the bedrock depth. Such a modest change
465 in average V_s , however, may be accompanied to strong layer-wise variations. The latter
466 consideration, points in the direction that Ibs-von Seht and Wohlenberg's approach is very
467 robust when the subsurface abides by the basic assumptions of the method.

468 It is noteworthy that for a normally dispersive subsurface, an increased V_s at depth leads to an
469 underestimation of sediments thickness while when the V_s at depth is decreased, the sediment
470 thickness is overestimated. However, in all the cases I investigated (i.e. layer-wise perturbation
471 up to 50%, resulting in an average V_s change under 20%), when the deviation of average V_s is
472 reasonable, the error is always below 20%. No simple relation between the deviation of the
473 average V_s and the error in estimation of the bedrock depth could be found, however, the
474 simulation approach herein proposed represents a useful tool to evaluate the reliability of a
475 bedrock depth estimated from real data. Such a tool accompanied by the H/V inversion enables
476 one to assess the reliability of the estimated depth through the stochastic investigation of the
477 parameters space around the reference model and may reveal a very convenient tool when
478 lateral variations are suspected or the number of available wells is not sufficient to obtain a
479 good regression. The opportunity of using the modeling/inversion tool for such purposes will
480 be discussed in a forth coming paper.

481 **5 Acknowledgements**

DOI: [10.1016/j.jappgeo.2017.07.017](https://doi.org/10.1016/j.jappgeo.2017.07.017)

482 The author would like to thank Prof. Giovanni Santarato, Prof. Riccardo Caputo, both at the
483 University of Ferrara (Italy) for their useful suggestions and for the stimulating discussions on
484 the topic and Ph. D. Robin Yezzi for the preliminary revising.

485

486 **Acknowledgements**

487 The author would like to thank Prof. Giovanni Santarato, Prof. Riccardo Caputo, and Prof.
488 Nasser Abu Zeid, at the University of Ferrara (Italy) for their useful suggestions and for the
489 stimulating discussions on the topic, and Ph. D. Robin Yezzi for the preliminary revising.

490

491 **References**

492 Abu Zeid, N., E. Corradini, S. Bignardi, V. Nizzo, G. Santarato (2017). The Passive Seismic
493 Technique 'HVSr' as a Reconnaissance Tool for Mapping Paleo-soils: The Case of the Pilastri
494 Archaeological Site, Northern Italy, Archaeological Prospection, DOI: 10.1002/arp.1568.

495 Abu Zeid, N., E. Corradini, S. Bignardi, G. Santarato (2016). Unusual Geophysical Techniques
496 in Archaeology - HVSr and Induced Polarization, A Case History, in Proceedings of the
497 NSAG-2016, 22nd European Meeting of Environmental and Engineering Geophysics, DOI:
498 10.3997/2214-4609.201602027.

499 Abu Zeid, N., S. Bignardi, R. Caputo, A. Mantovani, G. Tarabusi, and G. Santarato (2014).
500 Shear-wave velocity profiles across the Ferrara arc: a contribution for assessing the recent
501 activity of blind tectonic structures, in Proceedings of the 33th GNGTS National Convention
502 1117-122.

DOI: [10.1016/j.jappgeo.2017.07.017](https://doi.org/10.1016/j.jappgeo.2017.07.017)

503 Bard, P. Y. (1998). Microtremor measurement: a tool for site effect estimation?, in Proceedings
504 The Effects of Surface Geology on Seismic Motion, Yokohama Japan 3 1251-1279.

505 Bignardi, S, A. Mantovani, and N. Abu Zeid (2016). OpenHVSR: Imaging the subsurface
506 2D/3D elastic properties through multiple HVSR modeling and inversion, Comput. Geosci.
507 **93**(1) 103-113 DOI: 10.1016/j.cageo.2016.05.009.

508 Bonnefoy-Claudet, S., C. Cornou, P. Y. Bard, F. Cotton, P. Moczo, J. Kristek and F. Donat
509 (2006). H/V ratio: a tool for site effects evaluation. Results from 1-D noise simulations,
510 Geophys. J. Int. **167**(2) 827-837 DOI: <https://doi.org/10.1111/j.1365-246X.2006.03154.x>.

511 D13.08 (2004), Nature of wave field. Deliverable of the SESAME European Project, 50 pages.
512 (Available on the SESAME website : <http://SESAME-FP5.obs.ujf-grenoble.fr/>).

513 D23.12 (2005), Guidelines for the Implementation of the H/V Spectral Ratio Technique on
514 Ambient Vibrations Measurements, Processing and Interpretation, Deliverable of the
515 SESAME European Project, 62 pages, April 2005. (Available on the SESAME web site :
516 <http://SESAME-FP5.obs.ujf-grenoble.fr/>).

517 D'Amico, V., M. Picozzi, D. Albarello, G. Naso, and S. Tropenscovino (2004). Quick
518 estimates of soft sediment thicknesses from ambient noise horizontal to vertical spectral ratios:
519 a case study in southern Italy, J. Earthq. Eng. **8**(6) 895-908.
520 DOI:10.1142/S1363246904001729.

521 Delgado, J., C. Lo'pez Casado, J. Giner, A. Estévez, A. Cuenca, and S. Molina (2000).
522 Microtremors as a Geophysical Exploration Tool: Applications and Limitations, Pure Appl.
523 Geophys. **157** 1445-1462.

DOI: [10.1016/j.jappgeo.2017.07.017](https://doi.org/10.1016/j.jappgeo.2017.07.017)

524 Garcia-Jerez A, F. Luzon, M. Navarro, and A. Perez-Ruiz (2006). Characterization of the
525 sedimentary cover of the Zafarraya basin, southern Spain, by means of ambient noise, Bull.
526 Seismol. Soc. Am. **96**(3) 957-967 DOI:10.1785/0120050061.

527 Gosar, A., and A. Lenart (2010). Mapping the thickness of sediments in the Ljubljana Moor
528 basin (Slovenia) using microtremors, Bull. Earthq. Eng. **8** 501-518 DOI:10.1007/s10518-009-
529 9115-8.

530 Guéguen, P., C. Cornou, S. Garambois, and Banton, J. (2007). On the Limitation of the H/V
531 Spectral Ratio Using Seismic Noise as an Exploration Tool: Application to the Grenoble Valley
532 (France), a Small Apex Ratio Basin, Pure Appl. Geophys. **164** 115–134 DOI:10.1007/s00024-
533 006-0151-x.

534 Herak, M, (2008). ModelHVSR - A Matlab tool to model horizontal-to-vertical spectral ratio
535 of ambient noise, Comput. Geosci. **34** 1514–1526.

536 Hinzen K. G., F. Scherbaum , and B. Weber (2004). On the resolution of H/V measurements
537 to determine sediment thickness, a case study across a normal fault in the lower Rhine
538 embayment, Germany, J. Earthq. Eng. **8**(6) 909-926 DOI:10.1142/S136324690400178X.

539 Ibs-von Seht, M., and J. Wohlenberg (1999). Microtremor Measurements Used to Map
540 Thickness of Soft Sediments. Bull. Seismol. Soc. Am. **89**(1) 250-259.

541 Johnson, C. D., and J. W. Lane, (2016). Statistical comparison of methods for estimating
542 sediment thickness from horizontal-to-vertical spectral ratio (hvsvr) seismic methods: an
543 example from tylerville, connecticut, USA. The 29th Annual Symposium on the Application
544 of Geophysics to Engineering and Environmental Problems (SAGEEP), Denver, CO. March
545 20-24.

DOI: [10.1016/j.jappgeo.2017.07.017](https://doi.org/10.1016/j.jappgeo.2017.07.017)

546 Lachet, C., and P. Y. Bard (1994). Numerical and theoretical investigations on the possibilities
547 and limitations of Nakamura's technique, *J. of Phys. of the Earth* **42** 377-397

548 Lanzo, G., and F. Silvestri, (1999). *Risposta sismica locale. Teoria ed esperienze. Series:*
549 *Argomenti di ingegneria geotecnica. Avelius editions. 160 pp. EAN: 9788886977135 (Book*
550 *in Italian).*

551 Lunedei, E., and D. Albarello (2010). Theoretical HVSR curves from full wavefield modelling
552 of ambient vibrations in a weakly dissipative layered Earth, *Geophys. J. Int.* **181** 1093-1108
553 DOI: 10.1111/j.1365-246X.2010.04560.x.

554 Motamed, R., A. Ghalandarzadeh, I. Tawhata, and S. H. Tabatabaei (2007). Seismic
555 microzonation and damage assessment of Bam city, Southeastern Iran, *J. Earthq. Eng.* **11**(1)
556 110-132

557 Mucciarelli M., and M. R. Gallipoli (2001). A critical review of 10 years of Nakamura
558 technique, *Boll. Geof. Teor. Appl.* **42** 255-256.

559 Nakamura, Y., 1989. A method for dynamic characteristics estimation of subsurface using
560 microtremor on the ground surface, *Quarterly Report of Railway Technical Research Institute*
561 **30** 25-33.

562 Nakamura, Y. (2000). Clear identification of fundamental idea of Nakamura's technique and
563 its applications, in *Proceedings of the 12th World Conference on Earthquake Engineering.* 8
564 pp., New Zealand.

565 Parolai, S., P. Bormann, and C. Milkereit (2002). New relationship between V_s , thickness of
566 sediments, and resonance frequency calculated by the H/V ratio of seismic noise for the

DOI: [10.1016/j.jappgeo.2017.07.017](https://doi.org/10.1016/j.jappgeo.2017.07.017)

567 Cologne area (Germany), Bull. Seismol. Soc. Am. **92**(6) 2521-2527
 568 DOI:10.1785/0120010248.

569 Tsai, N.C., (1970). A note on the steady-state response of an elastic half-space, Bull. Seismol.
 570 Soc. Am. **60** 795-808.

571 Tsai, N.C., and G.W. Housner (1970). Calculation of surface motions of a layered half-space,
 572 Bull. Seismol. Soc. Am. **60** 1625-1651.

573 Wilken, D., T. Wunderlich, B. Majchczack, J. Andersen, and W. Rabbel (2015). Rayleigh-
 574 wave resonance analysis: a methodological test on a Viking age pit house. Journal of Cultural
 575 Heritage **9** 357–366 DOI: 10.1002/arp.1508.

576 **Appendix A: Subsurface Models**

Layer	H (m)	Vp (m/s)	Vs (m/s)	Rho (?)	Qp	Qs
Sedimentary	40	600	250	1.8	n.a.	n.a.
Rocky h.s.	n.a.	2000	800	1.8	n.a.	n.a.

577 **Table A.1:** Properties of the sediments and rocky half space used in test 1 are listed. During
 578 modeling, the 40 meter thick sedimentary cover was subdivided into 5 layers each one 8 meters
 579 thick. For sake of comparison with analytical solution (equation 2), the model was considered
 580 purely elastic so that quality factors Q_p and Q_s were set up accordingly.

581

Layer	H (m)	Vp (m/s)	Vs (m/s)	Rho (?)	Qp	Qs
1	10	426.	267	1.8	30	15
2	20	1500	377.7	1.8	30	15
3	20	1500	454.9	1.8	30	15
4	25	1500	513.7	1.8	30	15
5	25	1500	563.3	1.8	30	15
6	25	1500	603.7	2	30	15
7	25	1500	638.0	2	30	15
8	25	1500	668.1	2	30	15
9	25	1500	695.1	2	30	15
10	25	1500	719.6	2	30	15
11	25	1500	742.1	2	30	15
12	25	1500	762.9	2	30	15

DOI: [10.1016/j.jappgeo.2017.07.017](https://doi.org/10.1016/j.jappgeo.2017.07.017)

13	25	1500	782.4	2	30	15
14	25	1500	800.7	2	30	15
15	25	1500	818.0	2	30	15
16	25	1500	834.3	2	30	15
17	25	1500	849.9	2	30	15
18	25	1500	864.8	2	30	15
19	25	1500	879.0	2	30	15
20	25	1500	892.6	2	30	15
21	25	1500	905.8	2	30	15
22	25	1500	918.4	2.2	30	15
23	25	1500	930.7	2.2	30	15
24	25	1508	942.5	2.2	30	15
25	25	1526	953.9	2.2	30	15
26	25	1544	965.0	2.2	30	15
27	25	1561	975.8	2.2	30	15
28	25	1578	986.2	2.2	30	15
29	25	1594	996.4	2.2	30	15
30	25	1610	1006.4	2.2	30	15
31	25	1626	1016.0	2.2	30	15
h.s.	n.a	4000	2500	2.5	n.a	n.a.

582 **Table A.2:** Visco-elastic subsurface properties used in test 2 to simulate a deep bedrock
583 scenario.

584

Layer	H (m)	Vp (m/s)	Vs (m/s)	Rho (?)	Qp	Qs
1	2.7778	330.2	206.4		30	15
2	2.7778	409.2	255.7	1.8	30	15
3	2.7778	461.2	288.2	1.8	30	15
4	2.7778	500	313.3	1.8	30	15
5	2.7778	1500	334.0	1.8	30	15
6	2.7778	1500	351.8	1.8	30	15
7	2.7778	1500	367.6	1.8	30	15
8	2.7778	1500	381.8	1.8	30	15
9	2.7778	1500	394.7	1.8	30	15
10	2.7778	1500	406.6	1.8	30	15
11	2.7778	1500	417.7	1.8	30	15
12	2.7778	1500	428.0	1.8	30	15
13	2.7778	1500	437.8	1.8	30	15
14	2.7778	1500	447.0	1.8	30	15
15	2.7778	1500	455.7	1.8	30	15
16	2.7778	1500	464.0	1.8	30	15
17	2.7778	1500	472.0	1.8	30	15
18	2.7778	1500	479.6	1.8	30	15
h.s.	n.a.	4000	2500	2.5	n.a.	n.a.

585

DOI: [10.1016/j.jappgeo.2017.07.017](https://doi.org/10.1016/j.jappgeo.2017.07.017)

586 **Table A.3:** Visco-elastic subsurface properties used in test 2 to simulate a shallow bedrock
587 scenario.

588

589

590

591

preprint